

# Slope 보상을 가진 벅 LED 구동기의 모델링 및 해석

김 만고, 정영석, 김 남호  
부경대학교

## Modeling and Analysis of Buck LED Driver with Slope Compensation

Marn-Go Kim, Young-Seok Jung and Nam-Ho Kim  
Pukyong National University

### ABSTRACT

A discrete time domain modeling for the current-mode-controlled buck LED driver is presented in this paper. Based on the modeling result, a root locus analysis for the buck LED driver with slope compensation is done to derive the stability boundaries of feedback gains.

### 1. Introduction

The luminous flux of LEDs is mostly determined by the LED forward current. The regulated constant current control is needed to achieve constant brightness of LEDs. In the current regulated converter like LED driver, the control signal  $v_c$  is not slow. Because there is no low pass filter for the output current. The instantaneous control signal  $v_c$  should be employed to describe the behavior of the duty-cycle modulator in the current regulated converter. State-of-the-art approach for designing the feedback loops cannot be used for the current regulation problem. Very little work has been done in the area of modeling and control to improve dynamic performance of the current regulated LED driver.

In this paper, the systematic discrete time domain approach is adapted to modeling and analysis for the duty-cycle-controlled buck LED driver shown in Fig. 1. Root locus analysis is employed to derive the stability boundaries.

### 2. Modeling of current-mode-controlled buck LED driver with slope compensation

$$\delta X_{k+1} = A \cdot \delta X_k + B \cdot \delta v_r \quad (1)$$

where

$$\delta X_{k+1} = [ \delta i_{k+1} \quad \delta v_{k+1} ]^T, \quad \delta X_k = [ \delta i_k \quad \delta v_k ]^T,$$

$$A = \begin{bmatrix} a_{11} & a_{12} \\ a_{21} & a_{22} \end{bmatrix}, \quad B = \begin{bmatrix} b_1 \\ b_2 \end{bmatrix},$$

$$a_{11} = 1 - \frac{1}{(1-D)} \frac{1+k_p+k_{ni}D}{(1+k_p+k_{ni}D/2+S_r)}, \quad a_{12} = \frac{1}{R_s} \frac{1}{(1-D)} \frac{1}{(1+k_p+k_{ni}D/2+S_r)},$$

$$a_{21} = R_s \frac{k_{ni}(k_{ni}D/2-S_r)}{(1+k_p+k_{ni}D/2+S_r)}, \quad a_{22} = 1 - \frac{k_{ni}}{(1+k_p+k_{ni}D/2+S_r)},$$

$$b_1 = \frac{1}{R_s} \frac{1}{(1-D)} \frac{1+k_p+k_{ni}D}{(1+k_p+k_{ni}D/2+S_r)}, \quad b_2 = \frac{k_{ni}(S_r-k_{ni}D/2)}{(1+k_p+k_{ni}D/2+S_r)},$$

$$D = V_o/V_i, \quad k_p = \frac{R_1}{R_2}, \quad k_{ni} = \frac{T_s}{R_2 C_1}, \quad S_r = \frac{M_e}{(V_o R_s/L)} \frac{D}{(1-D)} = S_{r0} \frac{D}{(1-D)}.$$

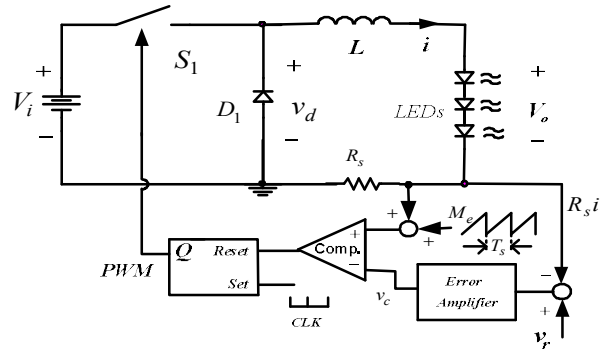


Fig. 1. Current-mode-controlled buck LED driver with slope compensation

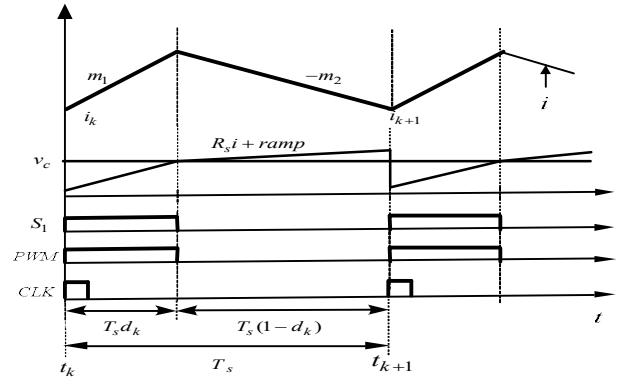


Fig. 2. Key theoretical waveforms of Fig. 1

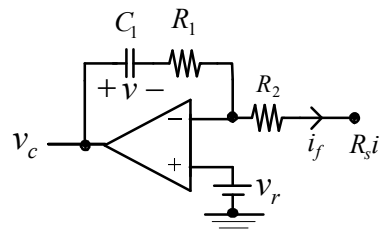


Fig. 3. Proportional-Integral error amplifier circuit

### 3. Analysis

Bode plots have been commonly used to assess the stability of the closed-loop system by finding the phase margin, but these plots cannot give information on the dynamic behavior of the individual state variables. On the other hand, root locus analysis can provide the engineer with the stability and the transient performance of the individual state variables related to the location of the roots of the characteristic equation.

To analyze the stability and dynamic characteristics of the closed-loop system, the eigenvalues of the system matrix is evaluated. The eigenvalues of A is the solutions of

$$|A - zI| = 0 \quad (2)$$

where I is the identity matrix. The following root locus analysis is performed for  $R_s = 1$ .

The root locus as a function of the integral gain  $k_{ni}$  for  $k_p = 0$ ,  $D=0.4$ , and  $S_{r0} = 1.19$  is shown in Fig. 4. The relationship between the s-plane poles and the z-plane poles is  $= e^{sT_s}|_{s=\sigma \pm j\omega} = e^{\sigma T_s} / \pm \omega T_s$ . When the I gain  $k_{ni}$  is increased from 0 to 0.49, the transient response is changed from overdamped to critically damped, and the overall system response becomes faster due to the slower eigenvalue  $\lambda_2$  moving towards the origin of the unit circle. The transient response is underdamped when the I gain  $k_{ni}$  is greater than 0.49. Selecting  $k_{ni}$  greater than 4.43, the closed loop system becomes unstable. In the unstable mode, the oscillation frequency is equal to half of the switching frequency.

Fig. 5 shows stability boundaries of  $k_{ni}$  as a function of D with increasing  $S_{r0}$ . When  $k_{ni}$  is between zero and the stability boundary, the closed-loop system is stable. The closed-loop system is unstable for the integral gain  $k_{ni}$  greater than the stability boundary. While the duty-cycle-controlled buck LED driver is always unstable for  $k_p = 0$ <sup>[7]</sup>, this CMC buck LED driver with slope compensation can be stable by selecting a proper I gain for  $k_p = 0$ . The stability boundary of  $k_{ni}$  is increasing with increasing  $k_p$  for  $D < 0.5$ . But, this stability boundary of  $k_{ni}$  is decreasing with increasing  $k_p$  for  $D > 0.5$ . The stable range of D becomes widened when  $S_{r0}$  is increased and  $k_p$  is decreased. When  $k_p$  is 0, the stable range of D between 0 and 1 can be designed if  $S_{r0}$  is greater than or equal to 0.9. Therefore, it can be said that the widest stable range of D can be obtained when  $k_p$  is 0.  $S_{r0}$  should be greater than or equal to 0.9 for the stable operation over all the operating area. However, the design engineer need to select the optimum  $k_{ni}$  for a good transient response.

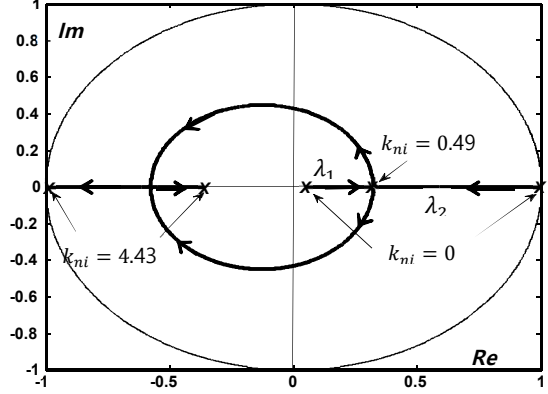


Fig. 4. Root locus as a function of  $k_{ni}$  ( $k_p = 0, D = 0.4, S_r = 0.79$ )

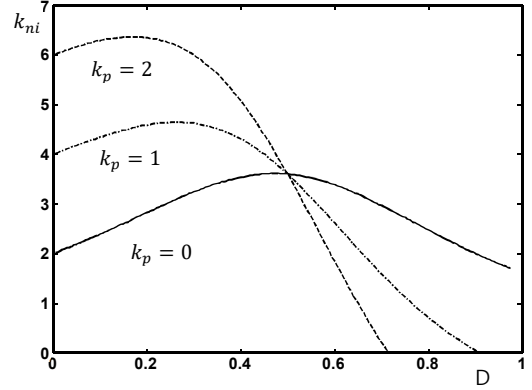


Fig. 5. Theoretical stability boundaries of  $k_{ni}$  as a function of D ( $S_{r0} = 0.9$ )

### References

- [1] R.D. Middlebrook, "Modeling Current-Programmed Buck and Boost Regulators," *IEEE Trans. Power Electron.*, vol. 4, no. 1, pp. 36-52, January 1989.
- [2] F.C. Lee, R.P. Iwens, Y. Yu, and J.E. Triner, "Generalized computer-aided discrete-time modeling and analysis of dc-dc converters," *IEEE Trans. Industr. Electron. Contr. Instrum.*, vol. IECI-26, no. 2, pp. 58-69, May 1979.
- [3] R.B. Ridley, "A new, continuous-time model for current-mode control," *IEEE Trans. Power Electron.*, vol. 6, no. 2, pp. 271-280, April 1991.
- [4] F.D. Tan and R.D. Middlebrook, "A unified model for current-programmed converters," *IEEE Trans. Power Electron.*, vol. 10, no. 4, pp. 397-408, July 1995.
- [5] Y.S. Jung and M.G. Kim, "Time-Delay effects on DC characteristics of peak current controlled power LED driver," *Journal of Power Electronics*, vol. 12, no. 5, pp. 715-722, Sept. 2012.
- [6] M.G. Kim, "Error amplifier design of peak current controlled (PCC) buck LED driver," *IEEE Trans. Power Electron.*, vol. 29, no. 12, pp. 6789-6795, Dec. 2014.
- [7] M.G. Kim, "Proportional-Integral (PI) compensator design of duty-cycle-controlled buck LED driver," *IEEE Trans. Power Electron.*, vol. 30, no. 7, pp. 3852-3859, Jul. 2015.
- [8] M.G. Kim, "High-performance current-mode-controller design of buck LED driver with slope compensation," DOI 10.1109/TPEL.2017.2671901, *IEEE Trans. Power Electron.*